CryoLetters 45(5), 269 – 278 (2024)

https://doi.org/10.54680/fr24510110112

PERSPECTIVE

CRYOSURGERY PROCESS APPLICATIONS: A MATHEMATICAL REVIEW

Lalhmingsangi Famhawite [1*], Sonam Tanwar [2] and Pooja Raj Verma [3]

[1]Department of Mathematics,
[2]Cluster Innovation Centre,
[3]Shaheed Bhagat Singh College,
University of Delhi, Delhi, India.
*Corresponding author's E-mail: lfamhawite@maths.du.ac.in

Abstract

The present study reviews some of the prominent mathematical models that are used to simulate the cryosurgery treatment of tumor tissues, i.e., destruction of tumor tissues via controlled freezing with cryoprobes with minimizing the impact on surrounding healthy tissues. Numerical simulation of the appropriate mathematical models that reflect practical situations may help the physicians to design a planning framework for the treatment, which includes total number of cryoprobes to be used, their placement design and the duration of optimal freezing, etc. Finite element method, meshfree method, and finite volume method are some of the suitable numerical techniques for simulating bio-heat transfer process within complex tissues during treatment.

Keywords: bioheat equation; double phase lag; necrosis analysis; numerical solution; phase transition; single phase lag; vascular network.

INTRODUCTION

Cryosurgery is a procedure that uses extreme cold to destroy abnormal tissues. Common cryogens include liquid argon, liquid nitrogen oxide, solid carbon dioxide and liquid nitrogen. Liquid nitrogen (boiling temperature -196°C) is the most effective cryogen. The duration and extent of the freezing has been studied widely. According to Cooper (1) who introduced modern cryosurgery, cellular destruction begins at –20°C. This temperature was later re-defined to –60°C by Neel et al. (2) and –70°C by Staren et al. (3). Based on certain in-vitro and clinical studies, it is accepted that cell destruction begins at –20°C

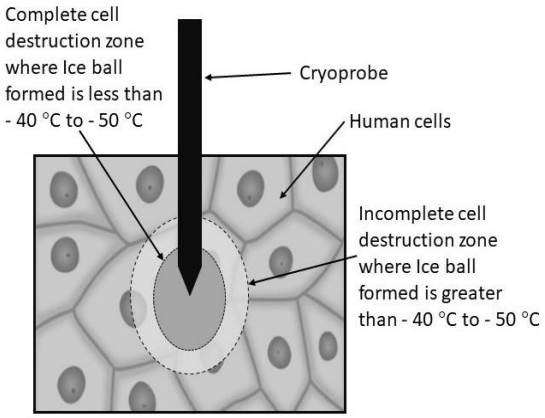

Figure 1. Schematic diagram of ice ball formed by single cryoprobe.

to –30°C, but complete destruction may not be achieved until –40°C or colder (4, 5, 6, 7). The schematic diagram of ice ball formation using cryoprobe in human tissue is given in Figure 1. Inappropriate freezing may not cover the whole required area or result in destruction of neighboring healthy tissues. To optimize cryosurgery, studies have been done to enhance cryo-process to achieve complete destruction of abnormal tissues and to minimize the injury of healthy tissues.

Cryosurgery has been used to treat skin conditions like warts, moles, solar keratose, and small cancers (8, 9, 10). It is also one of the effective cancer treatments for liver, prostate, lung, oral, etc. (11, 12, 13, 14, 15, 16). Although it is only appropriate against localized disease, other conditions such as plantar fasciitis and fibroma (17) can also be treated with cryosurgery. The advantage of cryosurgery and the reasons it is often preferred over conventional surgery is minimally invasive, low cost, minimal pain and anesthesia trauma, as well as good prognosis (4, 10, 18).

There are a number of factors for successful cryosurgery, including the understanding of cryosurgical mechanisms, thermal parameters, placement and number of cryoprobes required for optimal freezing, duration of freezing, etc. The numerical simulations with appropriate mathematical models may help the physicians to plan cryosurgical treatments. This review focuses on mathematical models and numerical solutions to bioheat equations in cryosurgery.

NOMENCLATURE

w_b	blood perfusion rate
k	thermal conductivity
k_u	thermal conductivity of unfrozen zone
K_f	thermal conductivity of frozen zone
ρ	density of tissue
ρ_b	density of blood
Q	heat source/sink
Q_m	heat due to tissue metabolism
L	latent heat
H	enthalpy function
V	velocity vector
g	gravity due to acceleration
∇_p	pressure gradient vector
μ_b	blood viscosity
T	heat flux relaxation in time
λ	heat flux relaxation in temperature gradient
T_1	temperature of melting/solidification begins
q	heat flux
q_b	heat transferred from blood to tissue
C	specific heat of tissue
C_b	specific heat of blood
C_{eff}	effective heat capacity
C_u	specific heat of unfrozen tissue
C_f	specific heat of frozen tissue
T	tissue temperature
T_b	arterial blood temperature
T_u	unfrozen tissue temperature
T_f	frozen tissue temperature
T_{ref}	reference temperature
T_0	body temperature
T_c	cryoprobe temperature
T_{dc}	cryogenic damage temperature
T_{nc}	cryogenic necrosis temperature
T_2	temperature where material totally melts

HISTORICAL ASPECTS

Cryosurgery deals with freezing of human tissues using extremely low temperature. In the

Table 1. Major events in the history of cryosurgery.

Time	Events
1845 - 1851	Arnott (19, 20) was the first physician to treat cancer by cooling.
1877	Systems for cooling gases is developed by Cailletet and Pictet (21).
1899	First clinical use of cryosurgery on skin diseases by White (22).
1907	First used of solid carbon dioxide by Pusey which easily freezes the skin lesion (23).
1950	First clinical application of liquid nitrogen by Allington (24) for treatments of verrucae, keratosis and various non-cancerous lesions.
1961	Cooper and Lee (1) first introduced cryosurgical probe using liquid nitrogen
1980s - 2000s	Modified cryoprobes and intraoperative ultrasound use, treatment of arterial diseases (21)
2001 - 2023	Computer simulations, cooling agents including nanoparticles, optimization of cryoprobes and wider studies on multiprobes (4,13, 31, 33).

middle of 19th century, Arnott treated cancer by freezing at low temperatures of –180°C to –240°C (19, 20). It developed over the years, and modern cryosurgery started in 1961 when Cooper and Lee, reviewed in (1), introduced their cryoprobe capable of freezing brain tissues and treatment of neural diseases. The probe was made up of three long concentric tubes, where the inner tube was supplied with liquid nitrogen from a pressurized source. The inner tube served as a conduit for liquid nitrogen to the flow of tip. Between 1980–2000 (21, 26, 27), due to further cryoprobe development, cryosurgery became an alternative therapy in cancer treatment. Furthermore, the combination of vacuum insulated cryoprobes with liquid nitrogen provided the super-cooling with temperature down to even –200°C.

In recent years cryosurgery is extended to treat arterial diseases and vascular tissues (11, 28, 29). Both experimental and numerical studies have examined the effect of cryogens, multiprobes, nanoparticle enhancement, front-tracking of the phase change transition, and optimal cryoprobe layout (4, 13, 30, 31, 32). Table 1 summarizes the major events in the history of cryosurgery.

CRYOSURGICAL MECHANISM

The mechanism of tissue destruction, size of freezing zone and thermal history within tissues are the most important factors during cryosurgery. The cryoprobe is brought into thermal contact with diseased tissues. Due to the internal circulation of cryogen, the diseased tissues in contact with probe is cooled to phase transition and to freeze. The heat in frozen tissues is either from blood circulation or metabolism of surrounding tissues. The tissues closer to the probe gets frozen first and gradually extends to the area further from the probe. Therefore, the rate of cooling depends upon several factors, such as the design and number of cryoprobes, cryogen used as well as tissue type.

Cryosurgery depends on two destructive mechanisms, acute or immediate damage and delayed tissue damage. Acute damage is caused by direct destruction via freezing (intra- and extracellular ice formation), while delayed damage results from blood vessel destruction and immune responses after surgery. Thermal history is briefly discussed below and a detailed discussion can be found elsewhere (18, 34, 35, 36).

Cooling effect

For a short period of time, most mammalian cells and tissues can endure non-freezing low temperatures, and they have adapted to the temperature range in which the organism lives. The cell membrane is responsible for the transport of chemical species in and out of the cell. Generally, the bilayer lipid membrane is semi-impermeable except that the membrane proteins allow mass transfer to occur. The lipid transforms into a gel phase or structures with lower free energy at lower temperatures, which causes the cell membrane to be more permeable and allows ions to enter the cell easier. The ionic composition in the cell changes and leads to cellular damage. Another mechanism related to cooling is the alteration of cytoskeleton structures which depends on chemical bonds between the cell scaffold and membrane proteins. The decrease of temperature leads to mechanical damage as it weakens the chemical bonds.

During cryosurgery, it is not expected that tissues around the frozen region would be severely damaged due to cooling. The region beyond the frozen zone may be damaged for cells highly depending on their ionic content, in particular, heart and around arteries. The detail discussion is given in publications (34, 35, 36).

Freezing effect

In cryosurgery, during the freezing process, freezing begins in the exterior of the cell and the interior of the cell is unfrozen. Experiments have shown that at lower temperatures, cells shrink as the extracellular concentration increases. Mazur et al. (58) hypothesized that hypertonic extracellular solutions damage the cells. The percentage of dead cells in the tissue after freezing is more than the situation after exposure to a similar extracellular hypertonic solution. This leads to an assumption that mechanical interactions between cells and ice may contribute to cell death. The mechanism of rapid cooling and intracellular ice formation near the cryoprobe are responsible for complete destruction of cells (58). Freezing may also stimulate immunological injury as the immune system is sensitive about the damaged tissue. Another effect of freezing is that it causes dehydration of the cell which disrupts the vascular and connective tissues. This leads to tissue necrosis.

Thawing effect

The effect of thawing and warming is less studied as compared to cooling and freezing. Nevertheless, complete thawing before the start of another cycle determines the success of cryosurgery. During the thawing process, ice has a tendency to recrystallize which will further disrupt the extracellular space and the tissue structures. As ice melts, the extracellular solution can be briefly hypotonic, which lets the water enter the cells and causes the membrane to rupture. When the thawing process is rapid, some cells may remain hypertonic at body temperature which causes disruption of the metabolism and additional damage.

MATHEMATICAL MODELS

Heat transfer process of freezing in biological tissues is complex due to differences in tissue structures and functions. It requires mathematical models with assumptions simplified to model the basic properties and thermal status of tissues and the effects of the boundary and initial conditions.

Pennes bioheat model is the most commonly studied model due to its simplicity. According to Pennes, heat transfer in living tissues involves two sources: the heat produced by metabolism (Q_m) and the heat transferred from blood to tissue (q_b). In this model, the main assumption is that the rate of heat transfer between blood and tissue is proportional to the product of the volumetric perfusion rate and the difference between arterial blood temperature and local tissue temperature. The relationship can be expressed as:

$$q_b = w_b c_b (T_b - T) \quad [1]$$

The final Pennes bioheat model is expressed as:

$$\rho c \frac{\partial T}{\partial t} = k \frac{\partial^2 T}{\partial x^2} + c_b \rho_b w_b (T_b - T) + Q_m - Q \quad [2]$$

In cryosurgery, the cryoprobe works as the heat sink and many studies directly impose low temperature as the boundary condition on the cryoprobe's geometry (11, 12, 13, 29). It is seen that temperature falls down to the ideal temperature faster with direct imposition of the boundary condition.

The Pennes model however does not consider vascular networks and blood circulatory systems. Recently, Nazebian and Nabaei (11, 29) have studied the effect of vascular network when performing cryosurgery by adding to the existing model the convective heat transfer between vessels and tissues. The continuity and Navier Stokes equations mentioned below were solved for the fluid domain:

$$\nabla . \rho_b V + \frac{\partial \rho_b}{\partial t} = 0 \quad [3]$$

$$\rho \frac{DV}{Dt} = \rho_b g - \nabla p + \mu_b \nabla^2 V \quad [4]$$

Finally, the heat transfer equation is solved for the fluid domain coupled to the solid domain:

$$\nabla . k \nabla T_b = \rho_b c_b \left(\frac{\partial T}{\partial t} + V . \nabla T_b \right) \quad [5]$$

The Pennes Bioheat model is based on Fourier law leading to a parabolic equation having infinite speed of the heat flux where the heat flux is related to the temperature gradient

$$q = -k \frac{\partial T}{\partial x} \quad [6]$$

However, the flux propagates with finite speed in real systems. Relaxation (or lag) time needs to be considered and this leads to the formation of two bioheat models resulting in hyperbolic equations:

i. Single Phase Lag (SPL) approach where relaxation is considered only in heat flux time; and
ii. Double Phase Lag (DPL) approach where the relaxation is considered both in heat fluxand temperature gradient.

Single phase lag approach

Single phase lag model, the Maxwell-Cattaneo model, considers the lag in temperature flux with respect to time. Hence, the Fourier law in Eq. [6] can be modified by using Taylor series expansion as:

$$q(x, t + \tau) = q(x, t) + \tau \frac{\partial q(x,t)}{\partial t} = -k \frac{\partial T}{\partial x} \quad [7]$$

where τ is the heat flux relaxation time (i.e., phase lag parameter). Substituting the new value of heat flux q, the bioheat model becomes:

$$\tau \rho c \frac{\partial^2 T}{\partial t^2} + (\rho c + \tau c_b \rho_b w_b) \frac{\partial T}{\partial t} = k \frac{\partial^2 T}{\partial x^2} + c_b \rho_b w_b (T_b - T) + Q_m - Q \quad [8]$$

The resulting equation becomes hyperbolic. If the relaxation time τ = 0, then, the equation is reduced to the parabolic classic Pennes Bioheat model.

Double phase lag approach

As an extension of the Maxwell-Cattaneo approach, Tzou (37) established dual phase lag

where heat flux relaxation is considered both in time and temperature gradient. Using Taylor series expansion, the Fourier law in Eq. [7] in one dimension becomes:

$$q + \tau \frac{\partial q}{\partial t} = -k \frac{\partial T}{\partial x} - k\lambda \frac{\partial}{\partial t}\left(\frac{\partial T}{\partial x}\right) \quad [9]$$

Finally, using Eq. [9], the dual phase lag bioheat equation is expressed as:

$$\tau \frac{\partial^2 T}{\partial t^2} + \left(1 + \tau \frac{c_b \rho_b w_b}{\rho c}\right) \frac{\partial T}{\partial t} + \frac{c_b \rho_b w_b}{\rho c}(T_b - T) = \left(1 + \lambda \frac{\partial}{\partial t}\right) \frac{\partial T}{\partial x^2} + \frac{q_m}{\rho c} \quad [10]$$

Kumar et al. (15) applied DPL model to thermal transfer during lung cancer cryosurgery. Li et al. (38) studied the thermoelastic analysis of the tissue during cryosurgery and considered relaxation time. Kumar and Rai (10) have applied DPL for skin cancer cryosurgery with the non-dimensional approach to solve the model further.

Although SPL is widely used for materials having a non-homogeneous internal structure, high heat flux, etc., studies showed that SPL considers only the rapid heat transfer and ignores microstructure interactions and heat transfer at small scales (55). In order to accurately predict the temperature profile in medium having different layers like skin tissue, it is required to use the modified Pennes equation including SPL and DPL. Moreover, DPL requires less time to achieve steady temperature in comparison with SPL (56, 57).

PHASE TRANSITION MODEL

Cryosurgery undergoes phase transition when temperature falls in the range of -1°C to -8°C (11, 12). This process involves conduction in tissue, convection between blood and tissue, perfusion in micro vascular and metabolic heat generation which makes it quite complex and non-linear due to solid liquid phase interference. The entire domain is unfrozen in the initial stage with initial temperature of 37°C. Once freezing starts and temperature reaches 1°C, it becomes mushy. Beyond -8°C is termed as the frozen region. Metabolic heat generation is taken as zero in the mushy and frozen zones. Phase transition may cause instability in numerical simulation. Therefore, methods used to tackle the phase transition are discussed further below.

Effective heat capacity method

Most of the literature in cryosurgery (5, 11, 12, 33) considered an effective heat capacity technique for phase transition. It is also called the fixed domain method. In this method, both solid and liquid phases are treated as single continuous medium and a single differential equation may be used for both domains. The effective heat capacity of the material (C_{eff}) is directly proportional to the stored and released energy during the phase change and the specific heat. However, it is inversely proportional to the width of the melting or solidification temperature range. The effective heat capacity (C_{eff}) of the Phase Change Material during the phase change is (39)

$$C_{eff} = \frac{L}{T_2 - T_1} + c \quad [11]$$

Therefore, using the effective heat capacity method, Penne's equation in Eq. [4] changed to

$$(\rho C)_{eff} \frac{\partial T}{\partial t} = k \frac{\partial^2 T}{\partial x^2} + c_b \rho_b w_b (T_b - T) + Q_m - Q \quad [12]$$

where,

$$(\rho C)_{eff} = \begin{cases} \rho C_u & T_u < T \\ \dfrac{\rho C_u + \rho C_f}{2} + \dfrac{L}{T_u - T_f} & T_f \leqslant T \leqslant T_u \\ \rho C_f & T < T_f \end{cases}$$

$$k = \begin{cases} k_u & T_u < T \\ \dfrac{k_u + k_f}{2} & T_f \leqslant T \leqslant T_u \\ k_f & T < T_f \end{cases}$$

Here, the temperature bounded between $T_u = -1$°C and $T_f = -8$°C is the mushy region.

Enthalpy method

According to the enthalpy method (15, 40), the phase change front is not simultaneously tracked, but is derived from the calculated temperature. This is possible as the phase fronts are implicitly accounted for in the enthalpy definition in the partial differential equations, which cause weak formulations. The enthalpy function H is defined as the integral of heat capacity with respect to temperature and its general form is written as

$$H(t) = \int_{T_{reff}}^{T} C(T) dT \quad [13]$$

where T_{ref} is a reference temperature and C is heat capacity which depends on temperature.

The enthalpy function highly depends on the type of material considered in the problem (41). For cases where phase change occurs over a finite interval [T_f, T_u], the enthalpy function in Eq. [13] can be given as

$$H(t) = \begin{cases} \int_{T_f}^{T} C_f(T)dT, & T < T_f \\ \int_{T_f}^{T} C_\alpha(T)dT + \frac{L}{\Delta T}\int_{T_f}^{T} dT & T_f \leqslant T \leqslant T_u \\ \int_{T_f}^{T_u} C_\alpha(T)dT + L + \int_{T_u}^{T} C_f(T)dT & T > T_u \end{cases} \quad [14]$$

or,

$$H(t) = \begin{cases} C_f\,(T - T_f) & T < T_f \\ C_\alpha\,(T - T_f) + \frac{L}{\Delta T}(T - T_f) & T_f \leqslant T \leqslant T_u \\ C_\alpha \Delta T + Q_{lf} + C_u(T - T_u) & T > T_u \end{cases} \quad [15]$$

where,

$$C_\alpha = \frac{C_u + C_f}{2}, \quad \Delta T = T_u - T_f$$

Finally, Pennes equation is transformed to

$$\rho \frac{\partial H}{\partial t} = k\frac{\partial^2 T}{\partial x^2} + c_b \rho_b w_b (T_b - T) + Q_m - Q \quad [16]$$

With the following initial and boundary equations:

for $i = u,f$

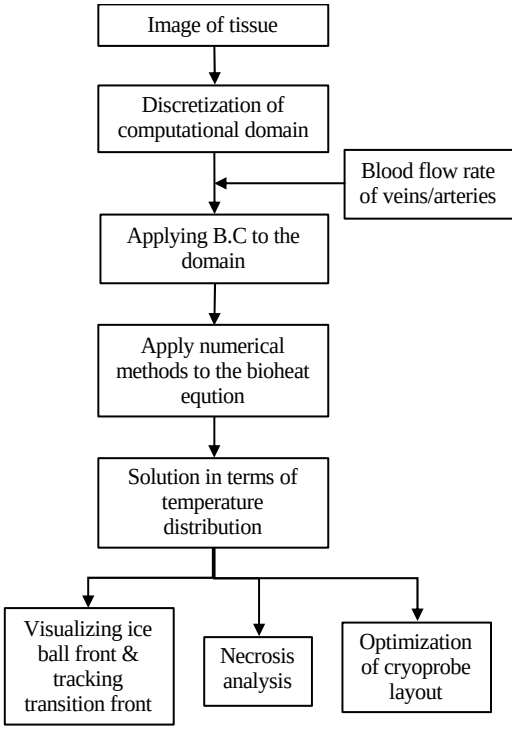

Figure 2. Flowchart of the numerical procedure.

$$T_i(x,t) = T_0\,, \quad at\ t = 0$$

$$\frac{\partial T_i(x,t)}{\partial t} = 0, \quad at\ t = 0$$

$$T_i(x,t) = T_c, \quad at\ x = 0$$

$$\frac{\partial T_i(x,t)}{\partial x} = 0, \quad at\ t = 0$$

Here, u, f stands for unfrozen and frozen domains respectively, T_0 is the body core temperature (37°C), T_c is the temperature of the cryoprobe used.

The two methods mentioned above solve the moving boundary conditions in phase transitions occurring in the freezing process. The instability and discontinuity in the phase transitions are taken care of with the modification of Pennes bioheat equation as shown in Eq. [12] (which utilize effective heat capacity method) and Eq. [16] (which utilize enthalpy method).

CRYOPROBE NUMBER AND OPTIMAL LAYOUT

The number of cryoprobes depends on the size and shape of the area to be treated. Table 2 displays some of the studies done. The position of multiprobes have a great impact on the efficiency of cryosurgery. Burkov et al. (32) have discussed the optimization of probe position and Jaberzadeh and Essert (31) compared different methods for preoperative planning of 3D liver cryosurgery using multiprobes.

NUMERICAL SOLUTIONS

Chua (4) has done an in vitro experimental setup using a storage tank consisting of a bio-gel. The experiment was used by others to validate the numerical results. The flow chart of the numerical procedure is given in Figure 2. The analytical approach may not be suitable to solve mathematical models due to the model being complicated in higher dimensions. Therefore, various numerical methods are applied to solve the mathematical models which are discussed as follows.

Numerical methods

To simulate cryosurgery, various numerical techniques are applied to the mathematical model. The finite volume method (46, 47), finite difference method (10, 48), finite element method (11, 14), extended finite

element method (X- FEM) (12), hybrid method (49, 50), α FEM (51), etc. are some of the advanced numerical techniques which have been used by different researchers. Using these methods, the mathematical models of Eq. [2], [3], [4], [5], [8], [10], [12] and [16] are solved for each iterative time steps which transformed the system of equations to algebraic equations. The numerical results give the temperature solution required for cryosurgical process. The methods and technique in detail were given in reports (10, 11, 12, 14, 46, 47, 48, 49, 50, 51).

The grid-based methods such as finite element and finite volume method require very fine mesh throughout the process otherwise the domain nearby the transition front needs to be re-meshed at each time step to capture the transition front accurately, while the mesh free method may take advantages of their arbitrary nodal distribution without fixed connectivity and nodes may be simply added or deleted at each step for accuracy. On the other hand, the fixed grid X-FEM may capture the evolving transition front accurately by identifying nodes with discontinuity and enriching them with the help of pre-defined enrichment functions.

Some of the software used for numerical simulation includes C^{++} (14), ANSYS (32), COMSOL (11, 33), IRENA (52) and MATLAB (12). Among these ANSYS and COMSOL are user friendly software which does not need the knowledge of computer programming and have inbuilt models for specific numerical problems. Another useful tool in simulating the numerical problem in COMSOL is the necrosis analysis discussed in the next section.

Tissue necrosis

To achieve complete tumor destruction by freezing, some surrounding healthy tissue is destroyed as well. Damage to the healthy tissue is caused by two things, the sudden cell death as the temperature falls below the cryogenic necrosis temperature (T_{nc}) or the slow cell death termed as cryogenic damage temperature (T_{dc}) that occurs when the tissue remains under a determined temperature for a certain time. T_{nc} and T_{dc} are considered to be -50°C and -20°C (1, 11, 29). Tissue necrosis is determined by the destruction index θ_d where the index value lies between 0 and 1. An index value closer to 1 indicates complete damage of tissue and 0 shows an undamaged tissue. COMSOL multiphysics has an inbuilt function under thermal analysis for the calculation of the destruction index θ_d as given by the following equation:

i) when tissue temperature is below T_{dc} for more than a specified period (t_{dc}):

$$\alpha_1 = \frac{1}{t_{dc}} \int_0^t (T < T_{dc}) dt \qquad [17]$$

ii) when tissue temperature drops below T_{nc}:

$$\alpha_2 = \int_0^t (T < T_{nc}) dt \qquad [18]$$

If $\alpha_2 > 0$, the tissue has reached the instant necrosis temperature and will be considered damaged. The overall θ_d by combining two cryogenic conditions is given as:

$$\begin{cases} \alpha_2 > 0 \;\; \theta_d = 1 \\ \alpha_2 < 0 \;\; \theta_d = min(1, \alpha_1) \end{cases} \qquad [19]$$

RISKS AND COMPLICATIONS

Although cryosurgery is considered to be a minimally invasive method, there are a number of risks and complications (53, 54) including:

i) acute blister formation, headache, pain;
ii) delayed infection, hemorrhage, cellulitis;
iii) prolonged hyperpigmentation, change of sensation; and
iv) permanent alopecia, hypopigmentation, keloids, scarring.

Therefore, a proper diagnosis must be made to determine the need of cryosurgery. Healing time correlates with the extent of freezing and may take longer depending on the tissues considered.

CONCLUSION

The mechanisms of cryoinjury can be complex and better understanding would likely have a greater impact clinically. Numerous current literature available have focused more on the numerical experiments considering regular shaped domains. Research in vivo experiment may be focused to define better the complexities of injuries caused by cryosurgery, or to analyze the effectiveness of cryosurgery in a human tissue which may be irregular in shape with complex vascular properties. Appropriate numerical methods may be used to simulate such experiments which gives temperature distribution across tissues useful for optimal preplanning of cryosurgeries for the placement of cryoprobes.

Table 2. Some studies on cryoprobe number and layout.

Reference(s)	Shape of tumor	Cryoprobes	Domain	Results and efficiency
Jankun et al. (1999) (42)	-	3	Prostate	Use of five or more probes for a short period of time is much more desirable for avoiding destruction of the gland.
Rewcastle (2001) (43)	-	1-5		The killing efficiency is measured by the ablative ratio (the volume enclosed by a critical isotherm divided by the total volume of ice ball). The ablative ratio increased to the maximum while single probe decreases continuously with respect to time.
Rossi et al (2007) (44)	-	6-14	Prostate	The increase in grid size of the domain results in lag of the freezing front. The increase in number of cryoprobes decreases the simulation time.
Chua (2011) (4)	Irregular	3-12	Liver	Less inter-probe, distance results in more cell destruction of tumor.
Singh & Bhargava (2014) (13)	Circular	1	Liver	Probe is used as a heat sink and nanoparticles increased the freezing rate, control the size and growth of ice-crystals.
Mirkhalili et al. (2015) (28)	-	1 and 3	Liver	Average tissue temperature is reduced due to the increase in probe number.
Kumar et al. (2017) (15)	-	1	Lung	On increasing relaxation time, phase change interface position decreases and tissue temperature increases.
Nabaei & Karimi (2018) (29)	Circular	1	Liver	The effect of blood vessel is considered and results shows that the freezing procedure and the ice-ball formation rate becomes slower when the vessel diameter increases or when it is close to the tumor. Tissue destruction during the surgery has also been analyzed.
Khademi et al. (2019) (45)	Circular	1-4	Vascular tissue	The increase of probes widened the freezing zone with faster crystal formation and withdrawal of the lethal isotherm is not dependent upon number of probes.
Nazemian & Nabaei (2020) (11)	Circular	1	Skin	Cryoprobes are inserted in different positions between vascular network complexity. Cryoablation coveragerates and ice ball regularity analyzed the efficiency of the surgery. The presence of larger or closer vessels around tumors causes irregular ice balls and the thermal effect of the adjacent arteries reduces ice ball volume.
Kumare & Rai (2021) (10)	Circular	1	Skin	Multilayer tissue with different boundary conditions in the outer layers with time relaxation (SPL) is considered. The cryogen and cryoprobe insertion depth have significant results in the procedure.

REFERENCES

1. Cooper IS (1964) *Cryobiology* **1(1)**, 44–51.
2. Neel I, Bryan H, Ketcham AS & Hammond WG (1971) *Archives of Surgery* **102**, 45–48.
3. Staren ED, Sabel MS, Gianakakis LM, Wiener GA, Hart VM, Gorski M, Dowlatshahi K, Corning BF, Haklin MF, Koukoulis G (1997) *Archives of Surgery* **132**, 28–33.
4. Chua K (2011) *Computers in Biology and Medicine* **41(7),** 493–505.
5. Liu Z, Muldrew K, Wan R & Rewcastle J (2003) *Computer Methods in Biomechanics and Biomedical Engineering* **6,** 197–208.
6. Baust JG, Gage AA, Bjerklund Johansen TE & Baust JM (2014) *Cryobiology* **68**, 1–11.
7. Patil AA (2021) *Egyptian Journal of Neurosurgery*, **36,** 15.
8. Andrews MD (2004) *Am Fam Physician* **69**, 2365–2372.
9. Bosch G & Klein WR (2005) *Vet Ophthalmol* **8,** 241–246.
10. Kumar M & Rai K (2021) *International Journal of Thermal Sciences* **160,** 106667.
11. Nazemian S & Nabaei M (2020) *International Journal of Thermal Sciences* **158,** 106569.
12. Tanwar S & Kumari P (2020) *Computers Mathematics with Applications* **79(8),** 2119–2132.
13. Singh S & Bhargava R (2014) *Journal of Heat Transfer* **136(12),** 121101.
14. Yang B, Wan RG, Muldrew KB & Donnelly BJ (2008) *Finite Elements in Analysis and Design* **44(5)**, 288–297.
15. Kumar A, Kumar S, Katiyar V & Telles S (2017) *Computers in Biology and Medicine*, **84,** 20–29.
16. Yu CH, Lin HP, Cheng SJ, Sun A & Chen HM (2014) *J Formos Med Assoc* **113,** 272–277.
17. Allen BH, Fallat LM & Schwartz SM (2007) *J Foot Ankle Surg*. **46**, 75–79.
18. Fesseha H & Yilma T (2020) *CPQ Medicine* **10**, 1–18.
19. Arnott JM (1850) *The Lancet* **56,** 257–259.
20. Arnott JM (1851) *On the Treatment of Cancer by the Regulated Application of an Anesthetic Temperature*. J Churchill, London, 32 pp.
21. Cooper DSM & Dawber RPR (2001) *Journal of the Royal Society of Medicine* **94(4)**, 196–201.
22. White A (1899) *Medication Reconciliation*, **56**,109–112.
23. Pusey WA (1907) *Journal of the American Medical Association* **XLIX,** 1354–1356.
24. Allington HV (1950) *Calif Med* **72**, 153–155.
25. Pegg D (1996) *Cryobiology* **4(33)**, 484.
26. Grana L, Kidd J & Swenson O (1969) *Journal of Cryosurgery* **2(1)**, 62.
27. Yantorno C, Soanes WA, Gonder MJ & Shulman S (1967) *Immunology* **12,** 395–410.
28. Mirkhalili SM, Ahmad Ramazani SA & Nazemidashtarjandi S (2015) *Computers in Biology and Medicine* **66,** 113–119.
29. Nabaei M and Karimi M (2018) *Journal of Thermal Biology* **77**, 45–54.
30. Burkov I, Pushkarev A, Ryabikin S, Shakurov A, Tsiganov D & Zherdev A (2022) *International Journal of Refrigeration* **133**, 30–40.
31. Jaberzadeh A & Essert C (2015) *Mathematical Methods in the Applied Sciences* **39,** 4764–4772. doi: 10.1002/mma.3548.
32. Burkov I, Pushkarev A, Shakurov A, Tsiganov D & Zherdev A (2020) *International Journal of Heat and Mass Transfer* **147**, 118946.
33. Tanwar S, Famhawite L & Verma PR (2023) *Journal of Thermal Biology* **113**, 103531.
34. Rubinsky B (2000) *Annual Review of Biomedical Engineering* **2(1),** 157–187,.
35. Gage AA & Baust JG (2002) *CryoLetters*, **23,** 69–78.
36. Yiu WK, Basco MT, Aruny JE, Cheng SWK & Sumpio BE (2007) *Int. J. Angiol*. **16,** 1–6.
37. Tzou DY (1995) *Journal of Heat Transfer*, **117,** 8–16.
38. Li X, Luo P, Qin QH & Tian X (2020) *Journal of Thermal Stresses* **43(8)**, 998–1016.
39. Lamberg P, Lehtiniemi R & Henell AM

(2004) *International Journal of Thermal Sciences* **43(3)**, 277–287.
40. Abraham J & Sparrow E (2007) *International Journal of Heat and Mass Transfer* **50(13)**, 2537–2544.
41. Nedjar B (2002) *Computers Structures* **80(1),** 9–21.
42. Jankun M, Kelly TJ, Zaim A, Young K, Keck RW, Selman SH & Jankun J (1999) *Comput Aided Surg* **4(4)**,193–199.
43. Rewcastle JC, Sandison GA, Muldrew K, Saliken JC & Donelly BJ (2001) *Med Phys* **28,** 1125–1137.
44. Rossi MR, Tanaka D, Shimada K & Rabin Y (2007) *Computer Methods and Programs in Biomedicine* **85 (1)**, 41–50.
45. Khademi R, Mohebbi-Kalhori D & Razminia A (2019) *International Journal of Heat and Mass Transfer* **137**, 1001–1013.
46. Kudryashov NA & Shilnikov KE (2015) *Journal of Computational and Applied Mathematics* **290,** 259–267.
47. Das K & Mishra SC (2015) *Journal of Thermal Biology* **52**,147–156.
48. Patil HM & Maniyeri R (2019) *Thermal Science and Engineering Progress* **10**, 42–47.
49. Singh S & Bhargava R (2015) *International Journal of Numerical Methods for Heat Fluid Flow* **25,** 570–592.
50. Condino S, Cutolo F, Cattari N, Colangeli S, Parchi PD, Piazza R, Ruinato AD, Capanna R & Ferrari V (2021) *Sensors* **21(13),** p. 4450.
51. Liu G & Lam K (2009) *Computational Mechanics* **43**, 369–391.
52. Gallinato O, de Senneville BD, Seror O & Poignard C (2020) *Math. Model. Nat. Phenom.* **15**, 11.
53. Wood JR & Anderson RL (1981) *Arch Ophthalmol* **99,** 460–463.
54. Unger JG (2022) *Medscape*.
55. Ghasemi MH, Hoseinzadeh S, Heyns PS & Wilke DN (2020) *Computer Modeling in Engineering & Sciences* **122,** 399-414.
56. Verma R & Kumar S (2023) *Journal of Thermal Biology* **114,** 103575.
57. Chaudhary RK & Singh J (2023) *International Communications in Heat and Mass Transfer* **149**, 107094.
58. Mazur P, Leibo SP & Chu EHY (1972) *Experimental Cell Research* **71**, 345-355.